Bulletin of the

Seismological Society of America

Vol. 65 February 1975 No. 1

AN ARRAY OF STRONG-MOTION ACCELEROGRAPHS IN BEAR VALLEY, CALIFORNIA

BY RICHARD J. DIELMAN, THOMAS C. HANKS, AND MIHAILO D. TRIFUNAC

ABSTRACT

Fifteen strong-motion accelerographs, each with the capability of writing the WWVB absolute time code on the recorded accelerogram, have been deployed in an elliptical array, at a station spacing of several kilometers, along the San Andreas Fault in the Bear Valley region of central California. Ten accelerograms were obtained for the June 22, 1973, earthquake (M = 3.9), located near the center of the array. Preliminary analyses of these accelerograms support previous suggestions that the crystalline rocks of the Gabilan Range possess higher material velocities and lower intrinsic absorption than do the Cretaceous and Cenozoic sedimentary rocks northeast of the fault zone. These accelerograms clearly indicate that a strong-motion accelerograph array of this sort can provide the basic data for source mechanism, wave propagation, and local ground-motion studies for earthquakes with magnitudes as small as 3.5–4.0.

INTRODUCTION

This paper describes a new type of strong-motion accelerograph array currently operating in the Bear Valley region of central California and presents, in preliminary form, some data obtained from it for the first year's operation. This array, operated by the California Institute of Technology, is one element of a coordinated effort, involving also the University of California, Berkeley, the University of Nevada, and the University of Washington, to determine precise amplitude-frequency characteristics of the elastic radiation generated by intermediate magnitude earthquakes in the frequency range 0.025 to 25 Hz.

The San Andreas Fault in central California, between Parkfield and San Juan Bautista, is currently a zone of high seismicity in the intermediate magnitude range ($3 \lesssim M \lesssim 5$) and appreciable fault creep localized in a narrow zone identified as the present fault trace on geomorphological grounds. Within this section of the San Andreas Fault, a 40-km segment, approximately between San Benito and the Cienega Road Winery (Almaden) has produced 5 $M \geqq 5$ earthquakes, 13 $M \geqq 4.5$ earthquakes, and 45 $M \geqq 4.0$ earthquakes in the past 35 years (T. V. McEvilly and L. R. Johnson, unpublished data). The Bear Valley region is loosely defined as the southeastern half of this 40-km segment (Figure 1).

The Bear Valley strong-motion array consists of 15 SMA-1 strong-motion accelerographs, individually equipped with CS-60-P WWVB time code radio receivers. Instrument locations are shown in Figure 1 and station data are presented in Table 1. The array has been deployed symmetrically across the presently active fault trace which separates low material velocity, highly attenuating Cretaceous and Cenozoic sedimentary rocks northeast of and including the fault zone from the higher material velocity, less attenuating metamorphic and volcanic rocks of the Gabilan Range southwest of the fault zone (Boore and Hill, 1973; Kurita, 1973).

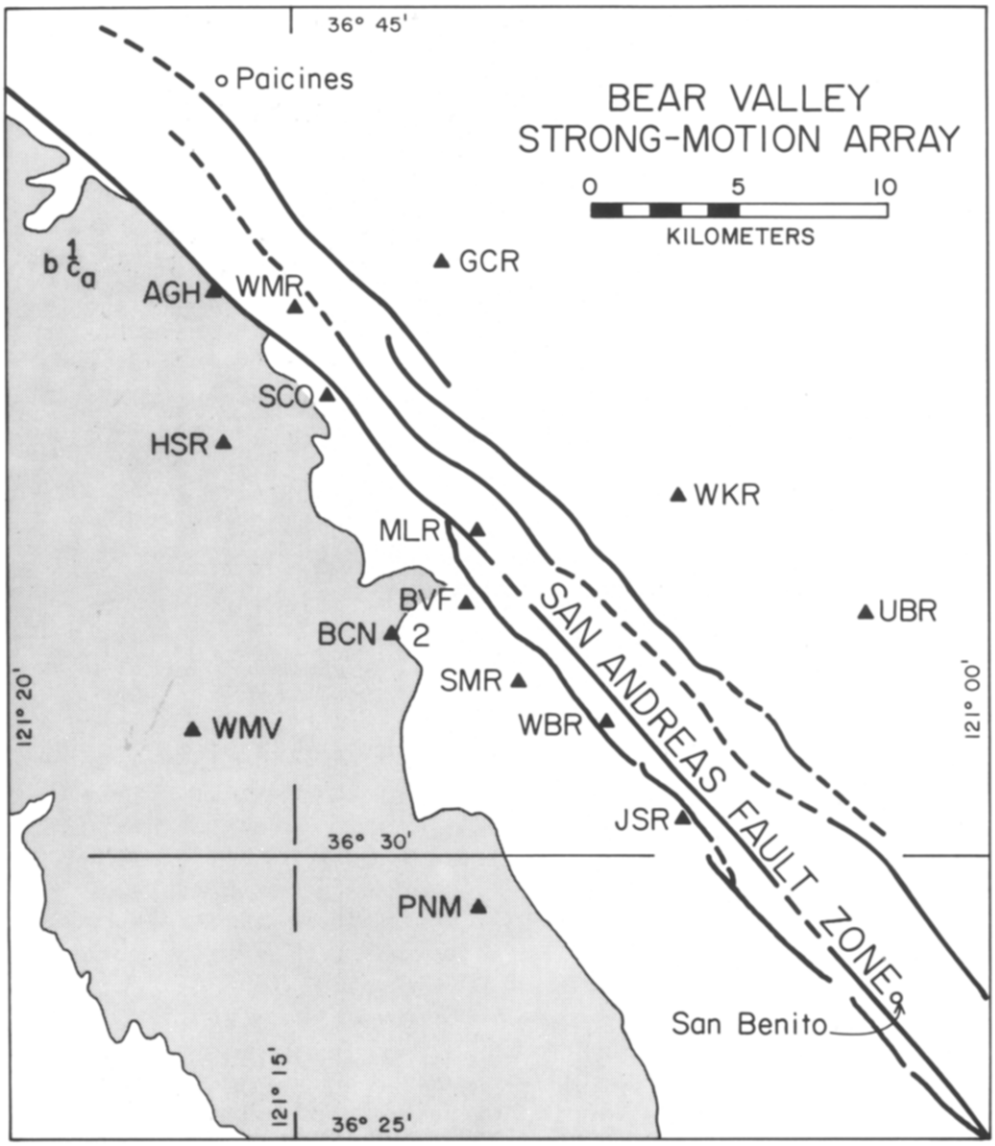

FIG. 1. Bear Valley strong-motion accelerograph array. Triangles indicate accelerograph sites identified with three-letter code (Table 1). Earthquake locations: 1. 011573 0943 $M = 4.2$, (*a*) 011573 1023 $M = 3.7$, (*b*) 011573 1024 $M = 3.3$, (*c*) 011573 1441 $M = 3.7$; 2. 062273 0129 $M = 3.9$ (Table 2). Stipled area marks exposed crystalline rocks at the Gabilan Range.

TABLE 1

STATION DATA

Station Abbr.	Station Name	Latitude, N	Longitude, W	Elevation	Geology	Installation Date
AGH	Almaden Winery Guest House	36°40.12′	121°16.60′	1250′	Pre-Cretaceous metamorphic rocks	9–20–72
BCN	Bickmore Canyon	36°33.95′	121°13.11′	1850′	Gabilan granite	9–24–72
BVF	Bear Valley Fire Station	36°34.35′	121°11.06′	1500′	Middle Miocene non-marine near contact with Quaternary alluvium	9–22–72
GCR	Callens Ranch	36°40.40′	121°11.70′	1050′	Plio-Pleistocene non-marine	9–23–72
HSR	Schrolls Ranch	36°37.30′	121°16.58′	2250′	Gabilan granite	9–24–72
JSR	James Ranch	36°30.24′	121°06.00′	1450′	Franciscan (red chert)	9–26–72
MLR	Melendy Ranch	36°35.55′	121°11.14′	1100′	Plio-Pleistocene non-marine	9–27–72
PNM	Pinnacles National Monument	36°28.99′	121°10.79′	1400′	Miocene volcanics	9–22–72
SCO	Stone Canyon Observatory	36°38.15′	121°14.03′	850′	Contact between Quaternary alluvium and Middle Miocene non-marine	9–27–72
SMR	Schmidt Ranch	36°33.10′	121°10.00′	1400′	Middle Miocene non-marine	9–28–72
UBR	Upper Butts Ranch	36°34.12′	121°02.60′	3000′	Lower Miocene marine	9–21–72
WBR	Webb Residence	36°31.09′	121°08.06′	1250′	Quaternary alluvium	9–27–73
WMV	Williamson Valley	36°32.80′	121°16.50′	2300′	Gabilan granite	12–16–73
WKR	Wilkinson Ranch	36°36.50′	121°06.55′	1950′	Plio-Pleistocene non-marine	9–25–72
WMR	Williams Ranch	36°39.48′	121°14.95′	750′	Quaternary non-marine	9–26–73

INSTRUMENTATION

The SMA-1 strong-motion accelerograph installed in the Bear Valley Array is entirely battery operated and utilizes a triaxial arrangement of accelerometers together with photo-optical recording. The accelerograph remains in a standby condition until a vertical starter senses a sufficient degree of ground motion (0.01 *g*, adjustable); it then activates a light source and film transport motor. The instrument reaches full operation 50 to 100 msec after being activated by the starter and continues to record as long as a motion of 0.01 *g* or greater is detected by the starter plus an additional 10 sec (adjustable). The accelerographs installed in Bear Valley have been modified to operate for a period greater than 60 sec in order for the WWVB time code to be received in its entirety. The 70-mm perforated photographic film is transported through a recording camera at a speed of 1 cm/sec. The 50-ft film supply enables the instrument to record approximately 25 consecutive events or record continuously for approximately 25 min.

The radio receiver used in Bear Valley is a solid-state, battery operated, portable unit (Figure 2) which receives a 60-KHz carrier signal transmitted by the National Bureau of Standards station, WWVB, in Fort Collins, Colorado. The 60-KHz carrier frequency is heterodyned with a beat frequency oscillator to produce an intermediate frequency of 2 KHz which is then applied to a code stripper, automatic gain control, and audio amplifier circuits. The sensitivity of the receiver is sufficient to receive the 60-KHz carrier

FIG. 2. Typical accelerograph installation with WWVB radio receiver mounted on top of strong-motion accelerograph.

signal at any point within the continental United States. The antenna used in conjunction with the radio receiver is a circular, wire-wound, loop antenna (Figure 3) tuned at 60 KHz.

All but three accelerographs of this array are located in government, state, or privately owned single-story structures, in conjunction with battery-float chargers when ac power is available. Three sites (HSR, BCN, and WMV) are fully external (Figure 3); the accelero-

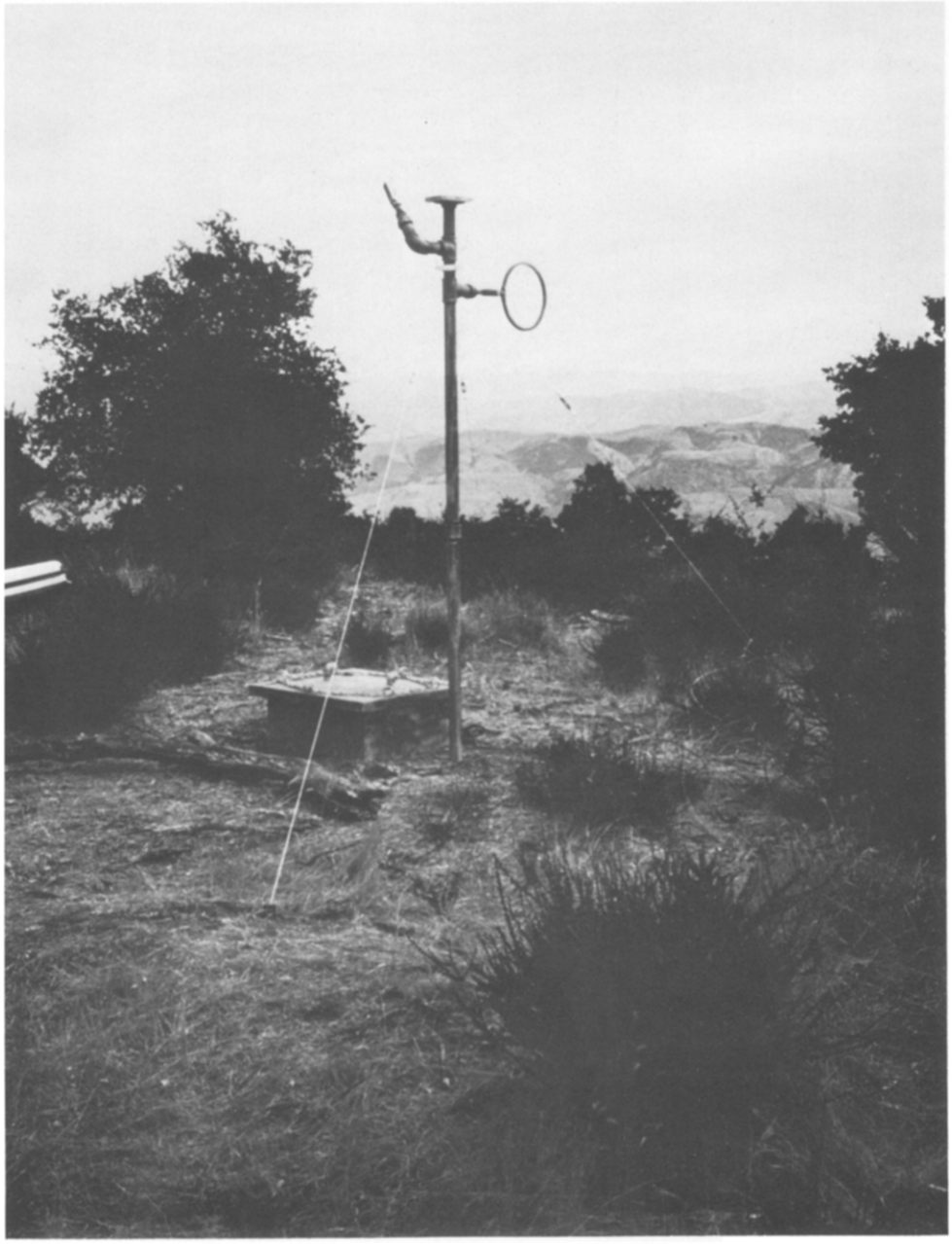

FIG. 3. External station of the array. The accelerograph and radio receiver are housed in the steel seismometer vault, with supporting pole for loop antenna and solar panels.

graph is housed in a steel seismometer vault, and batteries are charged with solar energy. The instrumental cost, at the time of installation, of a typical station of this array was approximately $1,800 (accelerograph, radio receiver, and antenna). When external siting

TABLE 2

EARTHQUAKE SOURCE* AND ACCELEROGRAM DATA

Date	Station	Origin Time	T	Latitude	S	Longitude	Depth (km)	M	Amplitudes (p–p in mm)		
									L	V	T
011573		0943:29.88		36°40.65′		121°18.75′	5.69	4.2			
	HSR		31.7		32.9				4	2 (P)	2
	BCN		33.2		35.1				<1	<1	<1
011573		1023:52.2		36°40.32′		121°18.49′	5.53	3.7			
	HSR		53.8		54.9				1.6	1.2 (P)	1.3
	BCN		55.1		57.2				<1	<1	<1
	GCR		55.5						<1	<1	<1
	AGH		56.0						<1	<1	<1
011573		1024:47.96		36°40.55′		121°19.06′	5.26	3.3			
	HSR		49.8 (P)		51.1				<1	<1	<1
011573		1441:22.31		36°40.56′		121°18.62′	6.01	3.7			
	HSR		24.2		25.3				2	1.0	1.2
	BCN		25.4		27.4				<1	<1	<1
062273		0129:12.2		36°33.80′		121°12.30′	9.5	3.9			
	BCN		14.0		15.1				2.1	1.2	2.1
	PNM		14.6		16.0				4.0	2.0	4.3
	JSR		15.0		17.1				1.5	<1	1.1
	WKR		16.2		17.1				2.6	1.2	2.2
	UBR		15.8		18.5				2.0	1.6	2.5
	GCR		15.8						<1	<1	<1
	BVF		15.5						1.0	<1	1.1
	SMR		16.1						1.1	1.0	1.5
	MLR		16.6						2.0	1.0	2.6
	HSR		16.6						<1	<1	<1

* USGS locations and magnitudes.

was necessary, an additional $350 was required for the seismometer vault and solar panels. Recent modifications of the radio receiver unit have allowed it to be housed within the accelerograph, at a slight reduction of cost for the instrumental package.

Accelerograph stations in Bear Valley have experienced severe climatic variations which to date have not affected their performance or reliability. During the winter months, temperatures are often as low as 0°F, and the higher elevations in the area usually experience light snowfall between November and March; conversely, summer temperatures are consistently in the 90° to 105°F range. Due to the reliability experienced during the 1st year's operation of the array, it is apparent that servicing intervals of 6 months will not significantly affect the performance of the instrumentation and have consequently been adopted.

Earthquake Accelerograms and Preliminary Results

As of October, 1973, 26 individual accelerograms have been obtained from the Bear Valley strong-motion array, 24 of which were recorded with the identifying WWVB radio signal. Of these, 12 record the earthquake 011573 0943 $M = 4.2$ and six identifiable aftershocks at as many as four stations, and ten record the earthquake 062273 0129 $M = 3.9$. For those earthquakes for which two or more accelerograms were taken, Table 2 summarizes earthquake source data and trigger (T) time, shear-wave (S) arrival time, and maximum amplitudes in millimeters as read on the original 70-mm film. Maximum accelerations may be estimated by dividing these data by the operating sensitivity (approximately 1.9 cm/g) and a factor of 2 to obtain zero-to-peak amplitudes. In addition, Table 2 summarizes these data for the earthquake 011573 1024 $M = 3.3$ recorded only at HSR.

The earthquake 011573 0943 $M = 4.2$ was recorded at HSR, with maximum accelerations of approximately 10 per cent g, and at BCN. Two aftershocks, 1023 $M = 3.7$ and 1441 $M = 3.7$, were recorded at two or more stations of the array. The aftershock 1024 $M = 3.3$ was recorded only at HSR, but this earthquake is significant because it was recorded within the run time of the accelerogram for 1023 $M = 3.7$. The epicenters of these earthquakes are shown in Figure 1. The accelerograms of 0943 $M = 4.2$ are displayed in Figure 4a and the accelerograms for 1024 $M = 3.3$ and 1441 $M = 3.7$ are displayed in Figure 4b. An aftershock with magnitude as small as 3.0 independently triggered the accelerograph at HSR.

Because 1024 $M = 3.3$ did not trigger the accelerograph at HSR independently, a true $S-P$ time (shear-wave arrival time minus P-wave arrival time) can be obtained for this earthquake. A comparison of this value with the $S-T$ times at HSR of the other earthquakes of this sequence indicates that the starting mechanism of the accelerograph is successfully triggering the instrument within 1/10 sec or so of the actual first motion for this particular source-station pair, even for earthquakes with magnitudes as small as 3.3.

Ten accelerograms were obtained for the earthquake 062273 0129 $M = 3.9$ (Figure 1, Table 2). The ten accelerograms are reproduced in Figure 5a and b. Maximum accelerations recorded for this earthquake were also in the range of 10 per cent g.

The five accelerograms of Figure 5a all triggered well in advance of the S-wave arrival, which is generally clear in these five accelerograms. The S-wave is sharpest at BCN and PNM, both of which are located in the crystalline rocks of the Gabilan Range, and is enriched in high-frequency ($\sim$10Hz) amplitudes at these stations relative to WKR and UBR northeast of the fault zone. The frequency content at JSR, which is located in the fault zone, is intermediate to these two extremes. The accelerogram obtained at GCR (Figure 5b) almost certainly triggered in advance of the S-wave arrival time (compare

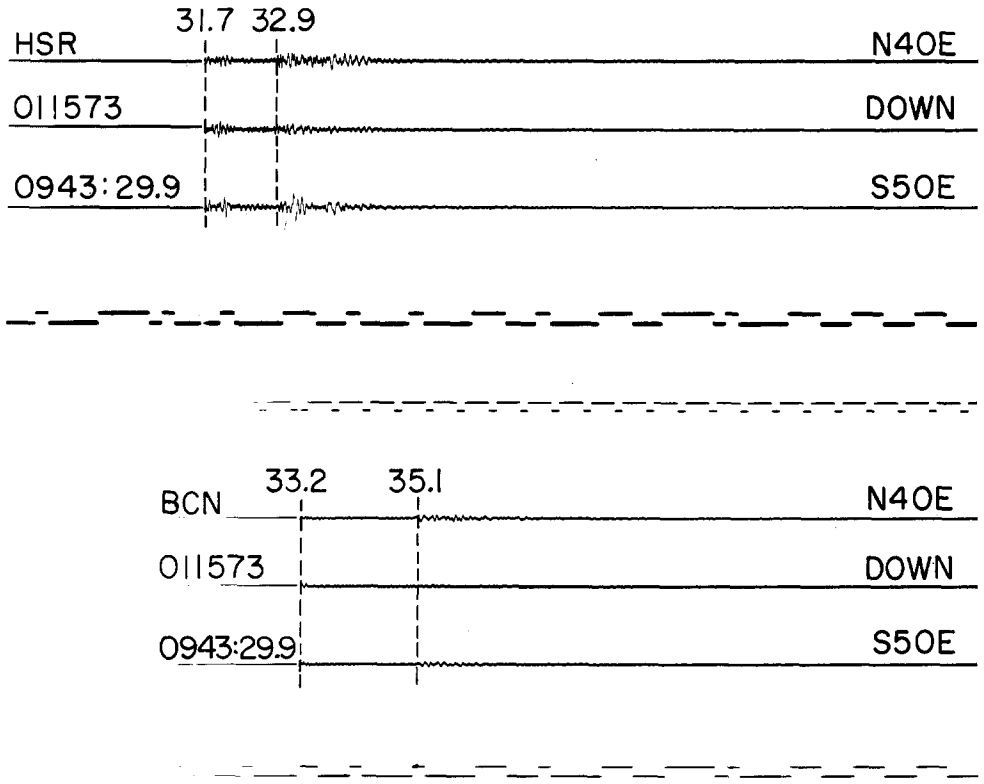

FIG. 4a. Accelerograms of 011573 0943 $M = 4.2$. T and S times are estimated with the vertical dashed lines; seconds and tenths of seconds in the minute of the earthquake are indicated.

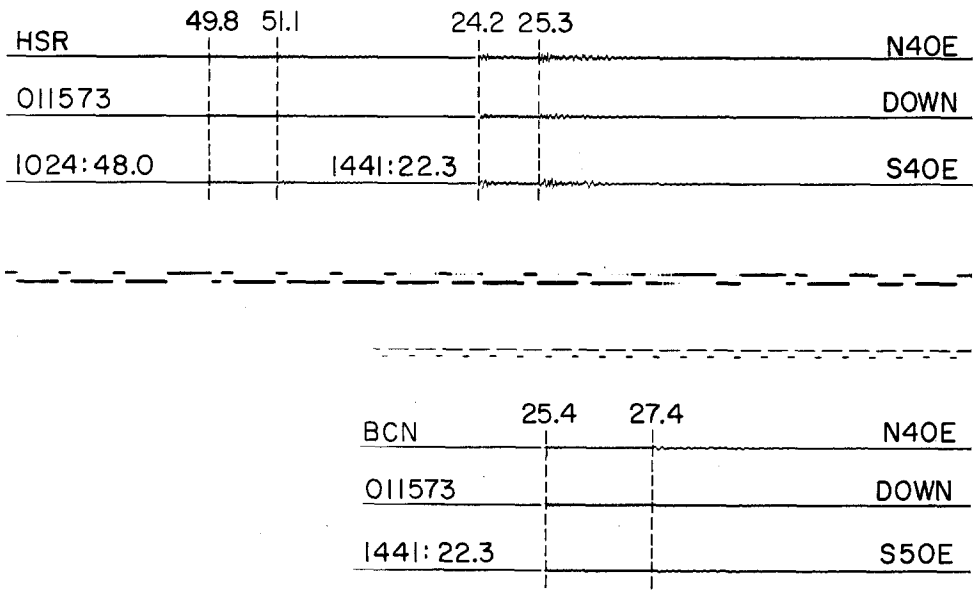

FIG. 4b. Accelerograms of 011573 1024 $M = 3.3$ with P and S times and 1441 $M = 3.7$ with T and S times.

trigger time and source-station geometry of GCR to those of the five accelerograms and stations of Figure 5b), but no clear identification of the S wave is possible at GCR. All of these observations are in accord with previous suggestions that transmission paths through the rocks northeast of the fault zone are more highly attenuating than paths through the crystalline rocks to the southwest of it (Kurita, 1973). Spectral analysis of these wave forms, however, will be necessary to verify this qualitative agreement, inasmuch as the longer duration of the shear-wave coda at JSR, UBR, and WKR may in part mitigate the clear difference in high-frequency excitation in the first $\frac{1}{2}$ sec of the S wave between these stations and BCN and PNM.

The distribution of trigger and S-wave arrival times at these five stations are consistent with the results of Boore and Hill (1973) that material velocities are significantly greater southwest of the fault zone than northeast of it. Table 3 summarizes travel-time residuals of computed P minus observed T and computed S minus observed S. As an hypothesis to be checked, we assume that the trigger time of the instrument will grossly correlate with the arrival of the P wave for these accelerograms, as the favorable comparison of the $S-T$ and $S-P$ times for the several events of the January 15 sequence at HSR has indicated. Residuals were computed with respect to the same velocity model used to obtain the USGS location (Table 2), and, of course, the trigger and S-wave arrival times reported here are independent of this location.

In Table 3, negative residuals indicate that the observed trigger or S-wave arrival time is early with respect to the computed P-wave and S-wave arrival, respectively, and positive residuals indicate the contrary. At BCN and PNM, the instrument triggered on or before the computed P wave, and the observed S waves arrive more quickly than the computed S waves. Both sets of residuals indicate that the actual compressional and shear-wave velocities are greater than those of the assumed velocity structure. At WKR and UBR, the opposite is true indicating actual compressional- and shear-wave velocities lower than those of the assumed velocity structure. Residuals at JSR, located within the

TABLE 3

TRAVEL TIME RESIDUALS OF 062273 0129 $M = 3.9$ AT FIVE STATIONS

Southwest	Fault Zone	Northeast
BCN $T = 0.00, S = -0.30$		WKR $T = 1.76, S = 0.94$
PNM $T = -0.8, S = -0.56$	JSR $T = 0.21, S = 0.35$	UBR $T = 0.73, S = 1.26$

fault zone, are intermediate to these two extremes, suggesting material velocities only slightly lower than those of the assumed velocity structure. For the four stations BCN, PNM, UBR, and JSR, the pattern of trigger time and S-wave residuals nominally supports the hypothesis that the trigger time is generally correlatable with the P-wave arrival time, but in the case of WKR, the trigger time is clearly late with respect to first motion.

CONCLUSIONS

The broadest significance of the earthquake accelerograms and preliminary results discussed in this paper lies simply in the fact that a large number of accelerograms of

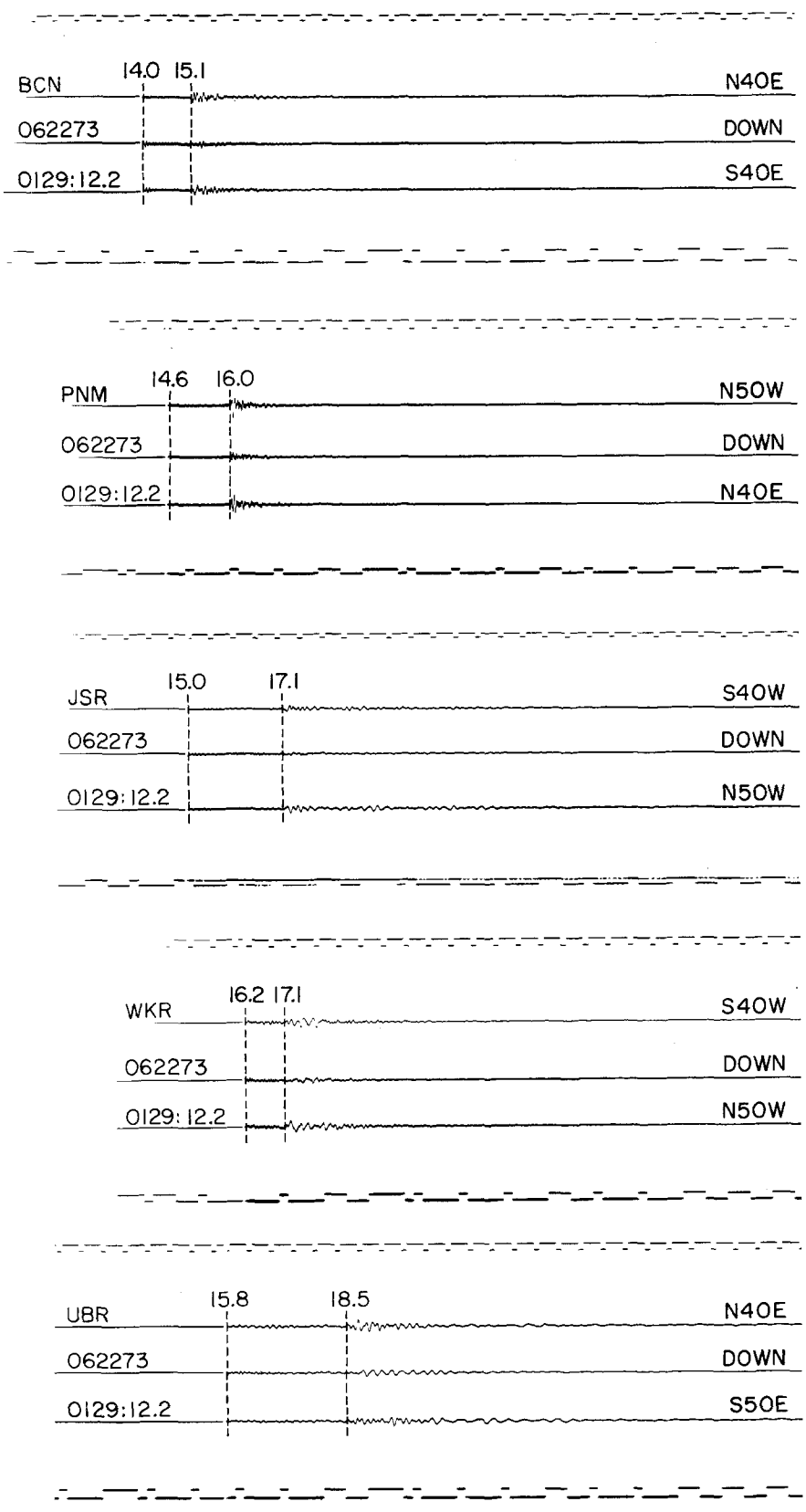

FIG. 5a. Accelerograms of 062273 0129 $M = 3.9$ with T and S times.

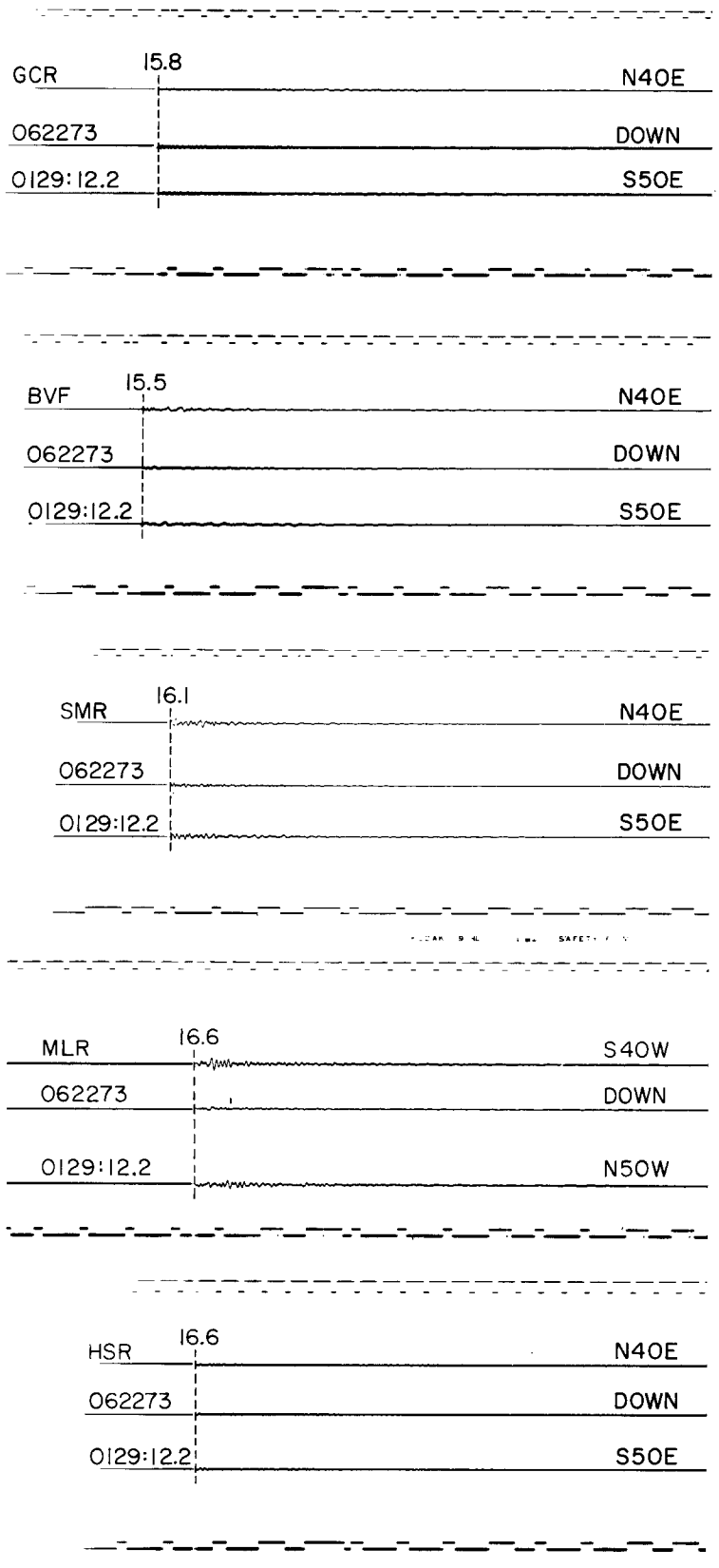

FIG. 5b. More accelerograms of 062273 0129 $M = 3.9$ with only T times given.

small magnitude earthquakes ($3 \lesssim M \lesssim 4$) have been obtained by a rugged, reliable, and very inexpensive network of strong-motion accelerographs. The strong-motion accelerograph, of course, was not designed for this purpose, but the instrumental capability of writing WWVB time code directly on the accelerogram together with a dense spacing (~ 5 km) of instruments will evidently allow for precise amplitude-frequency studies of small magnitude earthquakes in the frequency range of approximately 1 to 20 Hz at a number of recording sites. With appropriate modifications to accommodate local radio time codes, this strong-motion instrumentation system could be used throughout the world and would be particularly valuable in those regions where seismological and earthquake engineering investigations are yet in an embryonic stage. The accelerograms obtained for the 062273 0129 $M = 3.9$ earthquake bear ample witness to the capability of such a system to provide the basic data for source mechanism, wave propagation, and local ground-motion studies from earthquakes with magnitude as small as 3.5–4.0 over a relatively broad frequency range. Because of the rapid increase of the frequency of earthquake occurrence with decreasing magnitude, the potential scope of "strong-motion seismology" investigations has been considerably broadened.

Acknowledgments

We have appreciated the cooperation and patience of the property owners and local residents who have generously provided space for instrument installations: AGH, the Almaden Winery and Mrs. L. Dewitt; BCN, WMV, and MLR, Charlotte Berberick; BVF, Bear Valley Fire Station and Richard T. Gilbert; GCR, George H. Callens; HSR, Hannes Schroll; JSR, Mr. P. James; PNM, Pinnacles National Monument and Pat Patterson; SCO, Stone Canyon Observatory and Mr. R. Thompson; SMR, Jeff H. Schmidt; UBR, Charley Strohn; WBR, Mrs. L. E. Webb; WKR, Mr. F. Wilkinson; WMR, Thomas H. Williams. W. E. Ellsworth of NCER, U.S. Geological Survey, kindly provided the earthquake locations and determined the station residuals. We also thank the Seismic Engineering Branch of the U.S. Geological Survey for allowing us to incorporate three of their existing accelerograph stations into the Bear Valley strong-motion array.

This research was supported in part by the Advanced Research Project Agency of the Department of Defense and was monitored by the Air Force Office of Scientific Research under Contract F44620–72–C–0097 and by the Earthquake Research Affiliates Program of the California Institute of Technology.

References

Boore, D. M. and D. P. Hill (1973). Wave propagation characteristics in the vicinity of the San Andreas Fault, in *Proc. Conf. Tectonic Probl. San Andreas Fault System*, R. L. Kovach and A. Nur, Editors, pp. 215–223, *Stanford Univ. Publ., Univ. Ser., Geol. Sci.*, **13.**

Kurita, T. (1973). Attenuation of shear waves along the San Andreas Fault in central California, *Technical Report No. 2, AFOSR–72–2392, 2392A*, U.C. Berkeley.

Earthquake Engineering Research Laboratory
California Institute of Technology
Pasadena, California 91109

Manuscript received April 10, 1974.